J. Gibert
*Institut Paleontològic Dr M. Crusafont,
Carrer de l'Escola Industrial, 23,
08201 Sabadell, Barcelona, Spain*

P. Palmqvist
*Área de Paleontología, Departamento de
Geología y Ecología, Facultad de
Ciencias, Universidad de Málaga,
29071 Málaga, Spain*

Fractal analysis of the Orce skull sutures

Methods of fractal geometry (Mandelbrot, 1983) are used here to analyse the relative complexity of the sagittal and lambdoid sutures visible in the skull fragment formed by parts of an occipital squame and parietals found in a sealed deposit at the early Lower Pleistocene site of Venta Micena (Orce, Granada, Spain), generally regarded as human bone but occasionally suggested as belonging to an equid. For comparison with the fossil, corresponding sutures of various primates (hominids, pongids and cercopithecids) and two other groups of mammals (equids and ruminants) were analysed using the computer program FRACTAL-D (Slice, 1989) in order to determine their fractal dimensions as a measure of differential sutural design complexity. The results show that the fractal dimension of the Venta Micena skull sutures lies within the range of variation for infant specimens of both modern and Plio-Pleistocene hominids. Sutural complexity in young pongids and cercopithecids overlaps the range of fractal dimensions found in hominids, whereas values obtained from equids and ruminants are significantly greater than those for all the primates analysed here. Therefore, in terms of fractal dimension measures of relative complexity, the sutures preserved in the Venta Micena fossil could not have belonged to an equid (*pace* Agustí & Moyà-Sola, 1987); rather, its fractal dimension is consistent with the attribution of the fossil to an infant of *Homo* sp.

Introduction and background

The site of Venta Micena (Orce, Granada, southeastern Spain) lies in the northeast of the Guadix-Baza lacustrine basin. The fossils come from sediments cemented by micrite, which were deposited in outlying freshwater ponds surrounding a lake that then existed in the Orce valley (Vera *et al.*, 1985; Anadón *et al.*, 1987). The absence of sedimentary structures and preferred directions for elongated bones allows the rejection of geological processes in the formation of this assemblage.

The interspecific study of size/abundance patterns for ungulates excludes taphonomic biases, with exception of surface weathering processes prior to burial, which mainly affected those species of smaller body size (Palmqvist *et al.*, 1992). The results obtained in a factor analysis of correspondences (using as variates the frequencies of different skeletal elements in carnivore dens, rodent lairs and human assemblages) indicate that the main collecting agencies of bones in the Venta Micena site were probably hyaenids. A multivariate comparison with African biomass shows that this paleocommunity was similar in its faunal composition to that found in present day spiny tree and high grass savannahs (Mendoza *et al.*, 1993).

From 1982 onwards, systematic excavations at Venta Micena have provided some potential hominid fossils: an infantile cranial fragment, an infantile humeral diaphysis, and an adult humeral fragment. Our objective is to apply the methods of fractal geometry to the study of those sutures preserved in the skull; a preliminary version of some results obtained in this study have been published by Gibert & Palmqvist (1992).

Geology and age of the Venta Micena site

The fossils of Venta Micena are present in dark-coloured clayey palustrine sediments or in whitish calcareous levels that originally came from small freshwater ponds located in extensive emerged shorelines (calcimorphic paleosoils) (Anadón *et al.*, 1987; Gibert *et al.*, 1992).
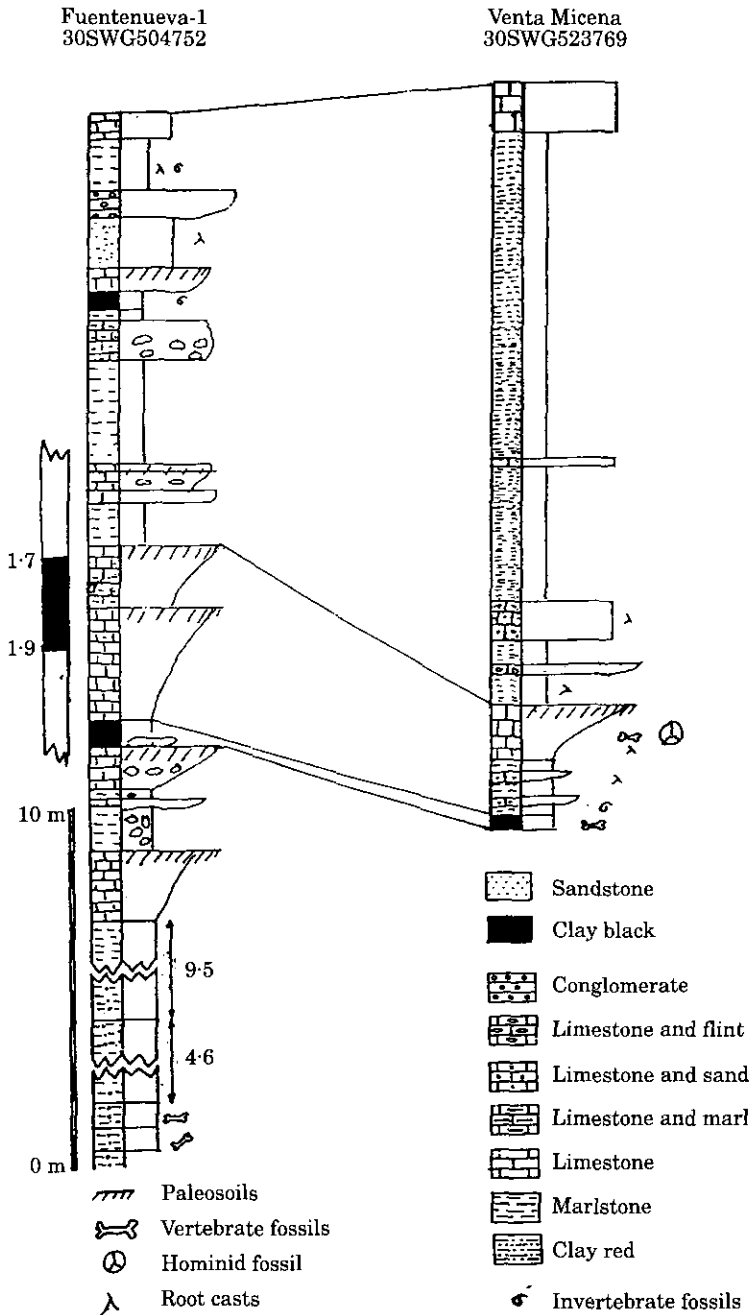
Figure 1. Paleomagnetic data of Venta Micena site.

In section Fuentenueva 1, the Olduvai event was situated in paleosoil levels 22 m from the Pliocene Fuentenueva 1 site (Gibert *et al.*, 1994). Correlations between this section and Venta Micena (Figure 1) were established in eight columns. The correlations between dark clayey levels and calcimorphic paleosoils were highly precise.
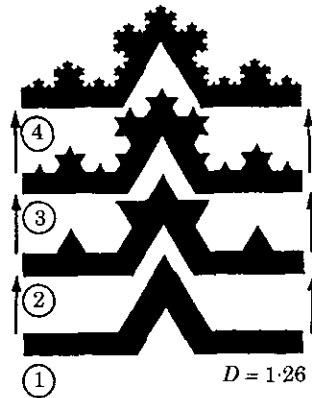
Figure 2. Four successive stages in the growth of von Koch's curve for a perfect fractal. A change of scale causes a segment made up of three parts to change into a segment formed by four parts in the next stage. For this reason, $D = \text{Log}(4)/\text{Log}(3) = 1\cdot 26$.

The location of the paleomagnetic inversion corresponding to the upper limit of the Olduvai event at the base of the Venta Micena paleosoil suggested an approximate age of $1\cdot 65$ m.y.a.

Fractal geometry

When we describe the world around us, we use one dimension to measure lines, two dimensions to measure surfaces and three to measure volumes. However, Euclidean geometry is insufficient to describe adequately many of the textures and structures that can be found in nature. This led to the development of a new geometry, known as fractal geometry (Mandelbrot, 1983), that employs fractional dimensions between one and two for complex curves, and between two and three for surfaces of complex texture. These new dimensions reflect the abstract mathematical concepts that a curve with dense curvature, like a winding river or a cranial suture, can nearly fill a plane, and a surface with intense folds like a mountain landscape, is almost equivalent to a volume. The mathematics and ideas behind fractals can be found in Barnsley (1988), Feder (1988) and Peitgen & Saupe (1988).

Estimation of fractal dimensions

Perfect fractal objects are self-similar. That is to say, their form is the same even if the scale used to observe them changes. To illustrate this, it is convenient to refer to a perfect or mathematical fractal, such as von Koch's curve, seen in Figure 2, which shows four successive stages of its development. To move from one stage to the next, the central thirds of every straight line are substituted by the side of an equilateral triangle that fits the gap exactly. It is possible to calculate its fractal dimension by treating each curve as a scaled-up version of the curve that is obtained from it when this procedure is followed. Each change of scale results in segments of curve that were made up of three parts, taking four parts in the next stage. This produces a fractal dimension of

$$D = \text{Log}(4)/\text{Log}(3) = 1\cdot 26 \quad \text{(see Mandelbrot, 1983)}$$

Structures which arise in nature do not, however, exhibit this perfect self-similarity of mathematical fractals. Rather, they tend to show a statistical regularity in their shape only

when they are examined over certain ranges of scale. Moreover, although the exact structural form is not invariant with a change of scale, broadly-speaking its relative complexity is preserved. The concept of fractal dimension can be used to both estimate and quantify the level of complexity of a natural structure and the closer we look at this, by raising the *magnifying-power of observation, the better we can inspect the complexity of the structure,* with corresponding consequences for our ability to estimate its length (Mandelbrot, 1967, 1983).

The commonest method of estimating the dimension of a fractal curve is the so-called "division method", which relies on measurements taken with compasses or dividers (Mandelbrot, 1983; Slice 1989, 1993; Sugihara & May, 1990; Reyment, 1991). The procedure is as follows. An initial reference point is chosen on the contour. An Euclidean distance is also selected as the step length, or unit of measurement. Starting from the initial reference point, a new point on the contour is found, such that the Euclidean distance between this new point and the reference point is equal to the step length. The new point now becomes the origin and the process is repeated until all the contour has been covered. For each step length, the estimated perimeter length is the sum of these Euclidean distances and if the distance between the last point of reference and the end of the contour exceeds half of the value of the unit of measurement, the estimated length is increased by the next multiple of the unit of measurement that has been employed.

There is an inverse relationship between the estimated contour length (*l*) and the unit of measurement employed (*e*), which can be linearized by means of a log-log transformation as in Equation (1)

$$\text{Log}(l) = a + b \ \text{Log}(e) \tag{1}$$

where *a*, the intersection with the vertical axis, is the log-length of the perimeter when the step length is equal to 1 and *b*, which is negative, is related to the fractal dimension (*D*) as follows,

$$D = 1 - b \tag{2}$$

The method of division with compasses, or dividers, is the one that is the most often used in order to estimate the fractal dimension. Slice (1989) has developed a computer program FRACTAL-D, which is easy to run. This program works on digitized contours. The (*x,y*) coordinates of any point on the contour are easily obtained using a digital tablet. For the Orce skull fragment, Figure 3 shows the perimeter estimations from two sutures combined—sagittal and right lambdoid sutures—with step lengths set at 4, 8 and 16 mm. As can be seen in Figure 3, the estimated perimeter lengths of 80, 72 and 64 mm with each step length, respectively, are inversely related to the scale of measurement used, and a linear relationship is obtained when both variables are expressed on a logarithmic scale. Other methods to calculate *D* are described by Morse *et al.* (1985), García-Ruíz *et al.* (1990) and Sugihara & May (1990).

Applications of fractal geometry

There are many applications of fractal analysis in scientific research and there is plenty of scope for further use of this approach. Some examples include the growth of crystals (Avnir *et al.*, 1984; Braddy & Ball, 1984; Sander, 1986), dynamic systems and chaos (Jakeman, 1984; Baker & Gollub, 1990), distribution of stratigraphical hiatuses (Plotnick, 1986, 1988), physiology and medicine (West & Goldberger, 1987; Caldwell *et al.*, 1990; Horsfield, 1990;
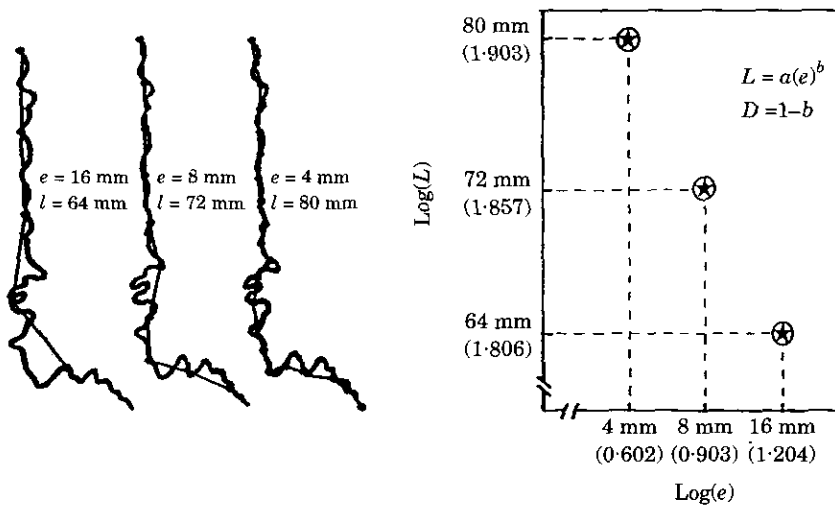
Figure 3. Estimation of fractal dimension of a curve (sagittal and right lamboid sutures of the Venta Micena skull fragment), on the basis of the inverse relationship between the scale of measurement used (*e*) and the perimeter length (*l*) estimated when this scale has been used.

Glenny *et al.*, 1991; Lynch *et al.*, 1991), shapes of landscapes and clouds (Burrough, 1981; Kent & Wong, 1982; Lovejoy, 1982), organic distribution patterns in ecology and biogeography (Loehle, 1983; Bradbury *et al.*, 1984; Morse *et al.*, 1985; Phillips, 1985; Pennycuick & Klein, 1986; Frontier, 1987; Dicke & Burrough, 1988; Caddy & Stamatopoulos, 1990), physiology (Sernetz *et al.*, 1985), botany (Vlecek & Cheung, 1986; Palmer, 1988; Tatsumi *et al.*, 1989), microbiology (Matsuyama *et al.*, 1989; Obert *et al.*, 1990; Ritz & Crawford, 1990) and taxonomy (Burlando, 1990), paleoclimatology (Fluegeman & Scott-Snow, 1989), shape of sedimentary grains (Hoyez, 1992), analysis of sutural design complexity in ammonites (Bayer, 1985; Boyajian & Lutz, 1992; Damiani, 1990; García Ruíz *et al.*, 1990; Cecca, 1992; Olóriz & Palmqvist, 1995), dynamics of extinctions in time-series analysis of fossil species abundances (McKinney & Frederik, 1992), and patterns of interfingering and interlocking seen in sagittal sutures of native American skulls (Hartwig, 1991). Without doubt, the discipline will experience rapid growth in coming years, and applications in different fields of knowledge will bring about methodological and conceptual transformations. Already, in the area of morphometrics Reyment (1991) believes that fractal geometry has opened up new horizons for the analysis of organic forms.

Fractals and intricate sutures

The form and dimensions of complex and intricate sutures, present both in the skulls of stags and in some ammonite shells, have been analysed by Long (1985). In ammonites, the septal sutures have a very long perimeter relative to the area of shell that they join, and they exhibit noteworthy "statistical" self-similarity when observed at varying scales of magnification. For both reasons, these sutures can be regarded as fractal curves.

García Ruíz *et al.* (1990) found that various species of Jurassic and Cretaceous ammonites have approximately the same complexity of sutural design with values of *D* around 1·37, some morphological differences in sutural form notwithstanding. This suggests the existence of a
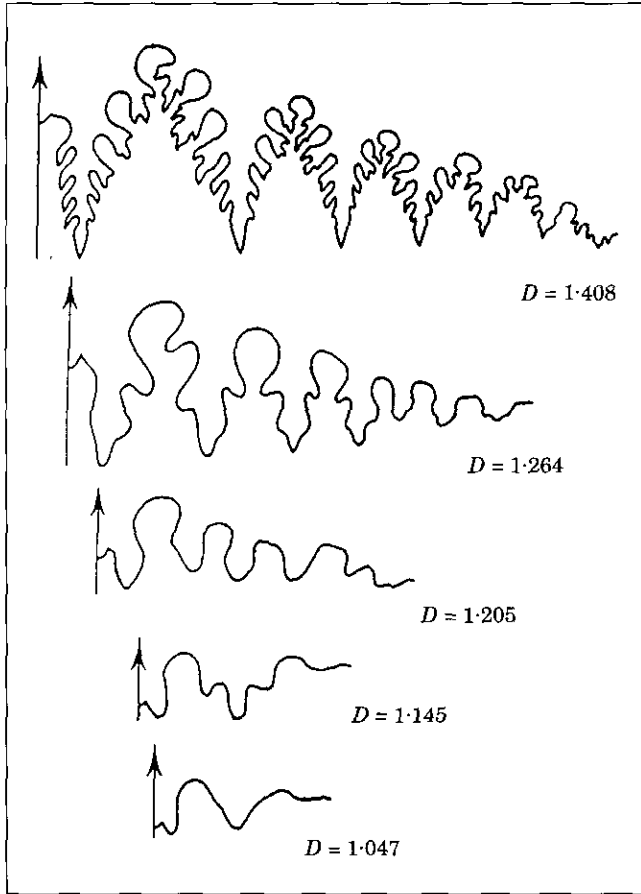
Figure 4. Successive stages in the ontogenetical development of the septal sutures of the ammonite *Perrinites hilli* (Smith), from the Permian period in Texas (redrawn from Moore, 1975, Figure 8). It can be seen that the progressive complexity in the design of sutures goes along with an increase in the fractal dimension (*D*).

common morphogenetical mechanism, perhaps characterized by a Saffman-Taylor type of instability (Nittman *et al.*, 1985). Olóriz & Palmqvist (1995) found in a study of Upper Jurassic ammonites that sutural complexity, as measured by fractal analysis, was related to shell structural types and degree of surface ornamentation. Figure 4 shows ammonite septal sutures corresponding to five successive ontogenetical stages in the development of the shell of *Perrinites hilli* (after Moore, 1975). Sutures are seen to become increasingly complex as the ontogeny evolves and folds become increasingly intricate, which is reflected in increasing values of the fractal dimension. Although apparent complexity is finally reached for the design of the suture, it is achieved through a simple generative pattern of the fractal type, similar to von Koch's curve (Figure 2). Mammalian skull sutures can also show high levels of complexity, especially in stags and bovids whose skulls have to bear weight or withstand stress, although levels of complexity are below those for septal sutures of most advanced ammonites. The fractal dimension of sutures can be used as a morphometrical descriptor of their relative complexity.

Material and methods

We used the fractal analysis of skull sutures in order to try to differentiate fragments of various mammalian species and in particular to solve the issue concerning the assignation to *Homo* of a posterior cranial fragment found during excavations at the early Lower Pleistocene site of Venta Micena near Orce in Granada, Spain (Gibert, 1986; Gibert *et al.*, 1986). Different lines of research point to its characteristically hominid morphology and immunology (Gibert *et al.*, 1989*a,b,c,d*; Campillo, 1989; Borja *et al.*, 1992). An alternative suggestion is that it might come from an equid skull (Agustí & Moyà-Solà, 1987).

Series of skull sutures were analysed in several different modern mammals and prehistoric and more ancient fossil hominids. Pongids, cercopithecids and ruminants, were obtained from the "Parque Zoológico de Barcelona" (Pongids: 32-2, 32-4, 33-3 and 34-2; cercopithecids: 250-1, 35-3, 35-1, 199-5, 68-1, 68-8, 108-1; ruminants: 4-20, 6-2, 47-3). Equids were obtained from the Hamburg University's Zoological museum (items 6933, 5444, 7476); EQACI specimen is situated in the "Institut de Paleontologia M. Crusafont" in Sabadell, Spain (see Table 1 and Figures 5 and 6).

Skull sutures in children between about 4 and 8 years old were analysed in a series from La Olmeda of 8th–12th century skulls (items 6, 38, 47 and 60), kindly made available by Drs D. Turbon and M. Hernández of the University of Barcelona, and in another from Illot de Porros of iron-age burials (item IP C-6 and IP C-37), kindly lent for study by Dr A. Malgosa of the Autonomous University of Barcelona (Table 1 and Figure 5).

Adult human skull sutures have been examined by A. Roca in a prehistoric skull with partially obliterated sutures (M.2) and in a series from Simia de N'Andreu (items SA 863, 864, 865, 866 and 868) and Bimidelfa (item BD 1) at the University of Barcelona. Other sutures considered are those accurately drawn and photographed in Gibert *et al.* (1989*d*). Skull sutures from some fossil hominids of Lower and Middle Pleistocene age (Black, 1930; Jacob, 1967; Stringer, 1974; Howell & Coppens, 1976; Tobias, 1991; Wood, 1991; Arsuaga *et al.*, 1993) were also analysed (see Table 1 and Figure 6). Zoukoudian specimens (items 1 and 2) are those photographed by D. Black in 1930 in his plates XI and XVI.

The computer program FRACTAL-D (Slice, 1989) was used to estimate the fractal dimension of cranial sutures. In order to facilitate comparison, all sutures were drawn at the same scale and were digitized using a CALCOMP digital tablet which permits a precision of 0·1 mm for taking Cartesian coordinates (x,y). The sagittal and right lambdoid sutures were analysed together for each skull because FRACTAL-D uses the "division method" (based on measurements taken with compasses or dividers) requiring an input of open or closed contours—it cannot work on bifurcating lines. For the Venta Micena fragment, the left lambdoid suture was discarded because it was smaller than the right.

It is necessary to explain that, although reliable comparisons between hominids and equids can be established for the cranial regions in question (Gibert *et al.*, 1989*a,c,d*), hominid and ruminant skulls are not directly comparable because bovid horns result in anatomical cranial differences. Comparisons between them can, however, be made if sagittal sutural patterns are taken to be equivalent to frontal ones, and lambdoid ones to coronal ones, from the standpoint of analysis of sutural fractal structure and relative sutural pattern complexity.

The fractal dimension of the sutures was estimated after taking step lengths of 1, 2, 3, 4, 6, 8, 11, 16 and 20 mm. The same step lengths were used in each case. The choice of this step length set was determined by the condition that, after taking logarithms, the points remained more or less equidistant on the x axis. The procedure was repeated with other step-length sets,

Table 1 Values of the fractal dimension (*D*) for cranial sutures from the specimens that were analysed. They are grouped by genus (Hominids, Pongids, Cercopithecids, Equids and Ruminants)

Specimens	Reference	Sex	Age	D
Orce skull	(Venta Micena)	—	—	1·058
Hominids				
Lower Pleistocene:				
Homo aff. H. erectus	KNMER-730B,D	—	Adult	1·037
Homo habilis	OH 13	—	Adult	1·042
Homo erectus	Sangiran 10	—	Adult	1·086
Australopithecus sp.	Omo, 338y	—	Infant	1·121
Middle Pleistocene:				
Homo erectus	Zoukoudian 1	—	Juvenile	1·071
Homo erectus	Zoukoudian 2	—	Juvenile	1·133
Homo sapiens archaic	Homo 2 (Kibish)	—	Adult	1·166
Homo sapiens archaic	Atapuerca 5	—	Adult	1·182
Homo sapiens archaic	Broken Hill	—	Adult	1·216
Homo sapiens archaic	Petralona	—	Adult	1·227
Modern:				
Homo sapiens sapiens	IP C-37	—	Infant	1·047
Homo sapiens sapiens	M.2	—	Adult	1·063
Homo sapiens sapiens	IP C-6	—	Infant	1·079
Homo sapiens sapiens	S.A. 868	—	Infant	1·099
Homo sapiens sapiens	6	—	4–6 years	1·138
Homo sapiens sapiens	S.A. 866	♂	Adult	1·145
Homo sapiens sapiens	47		5 years	1·146
Homo sapiens sapiens	60	—	6, 5 years	1·159
Homo sapiens sapiens	S.A. 863	♀	Adult	1·168
Homo sapiens sapiens	38	—	8 years	1·173
Homo sapiens sapiens	BD.1	♀	Adult	1·201
Homo sapiens sapiens	S.A. 864	♂	Adult	1·222
Homo sapiens sapiens	S.A. 865	♀	Adult	1·246
Pongids				
Gorilla gorilla	32-2	♀	Juvenile	1·074
Gorilla gorilla	32-4	♂	Juvenile	1·153
Gorilla gorilla	33-3	♀	Juvenile	1·082
Pongo pigmaeus	34-2	—	Juvenile	1·134
Cercopithecids				
Macaca fascicularis	250-1	♂	Juvenile	1·132
Macaca sylvana	35-3	—	—	1·141
Macaca sylvana	35-1	♂	Adult	1·183
Erithrocebus patas	199-5	♀	Juvenile	1·002
Mandrillus sp.	68-1	♀	Adult	1·003
Mandrillus sp.	68-8	♀	Adult	1·020
Papio hamadryas	108-1	—	—	1·006
Equids				
Equus przewalskii	6933	♂	0–1 months	1·123
Equus hemionus onager	5444	♀	3–4 months	1·249
Equus hemionus onager	7476	♀	5 months	1·322
Equus sp.	EQACI	—	8 months	1·374
Ruminants				
Cervus elaphus	4-20	♀	Juvenile	1·303
Elaphurus davidianus	6-2	♂	Adult	1·329
Cervicapra sp.	47-3	♀	Adult	1·186
Kobus defassa	300-1	♀	Adult	1·201
Capra alba	Fossil (V.M.)	—	—	1·297

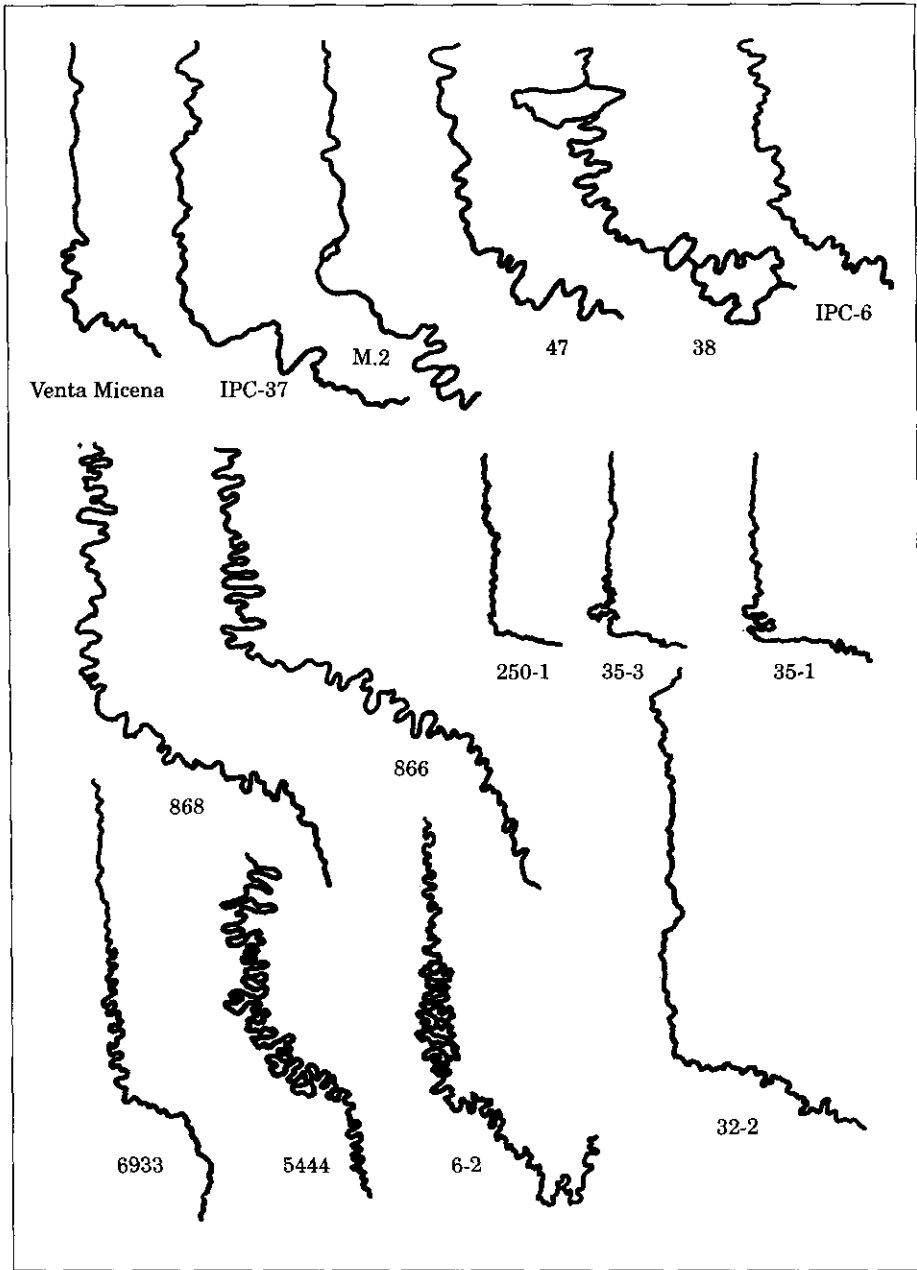Specimens are grouped by genus and the hominids are grouped by fractal dimension scores.

Figure 5. Sagittal and right lambdoid sutures from the Venta Micena fossil and some of the modern specimens analysed (drawn to half actual size). The values of fractal dimension that were calculated from these sutures are shown in Table 1.

but the results were in all cases very similar to those described here; this independence of scale is hardly surprising, given the remarkable self-similarity in fractal design of most of the cranial sutures studied.
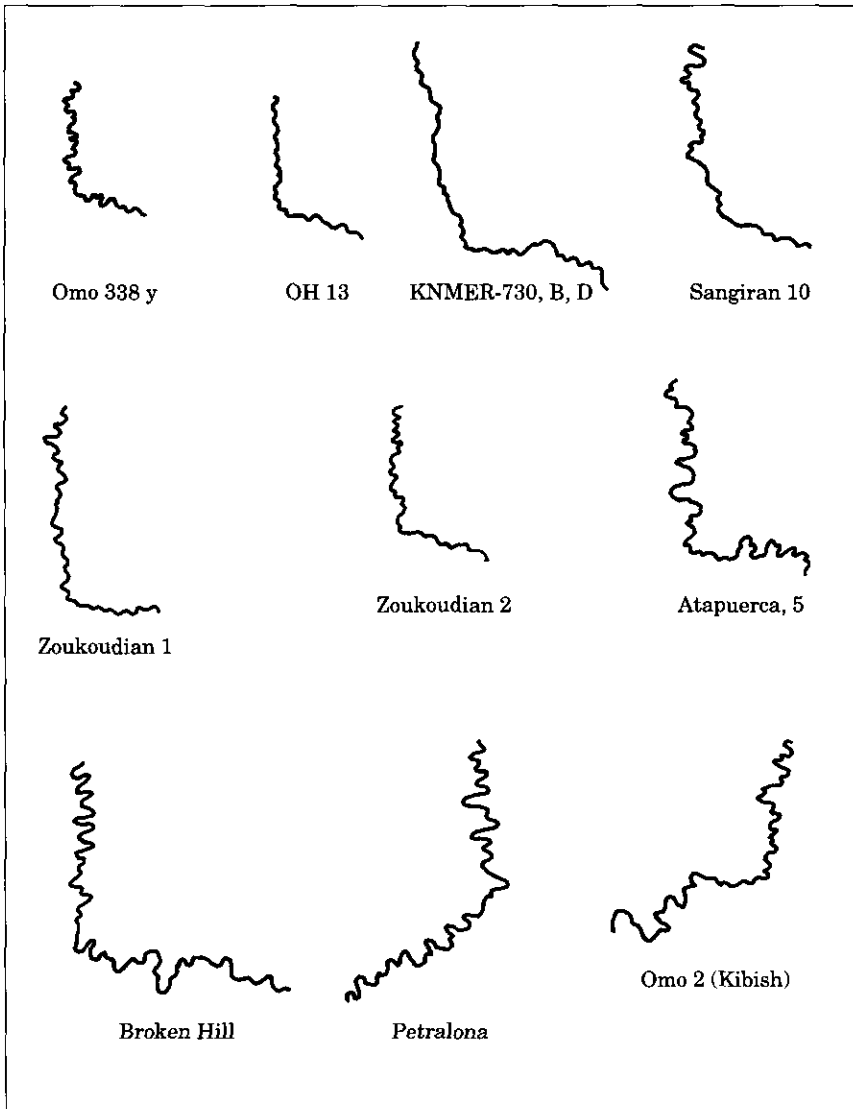
Figure 6. Sagittal and lambdoid sutures from hominids of Lower and Middle Pleistocene age (drawn to half actual size). Their values of fractal dimension are shown in Table 1.

The computer program FRACTAL-D calculates the fractal dimension, as established by Mandelbrot (1983), by adding the slope of the fitted curve for log-perimeter *vs.* log-scale to the topological or Euclidean dimension (one) of the sutures. Hartwig (1991) has applied a different method to the analysis of human sagittal sutures: a "structured walk technique", which provides a non-linear regression of values on a Richardson (log-log) plot where the distribution of points is polynomial and two slopes can be distinguished, but the point of inflection between them must be determined subjectively. Hartwig calls the fractal dimensions calculated from these slopes "textural" (Dt) and "structural" (Ds); our results can be compared to Hartwig's "textural" dimension.
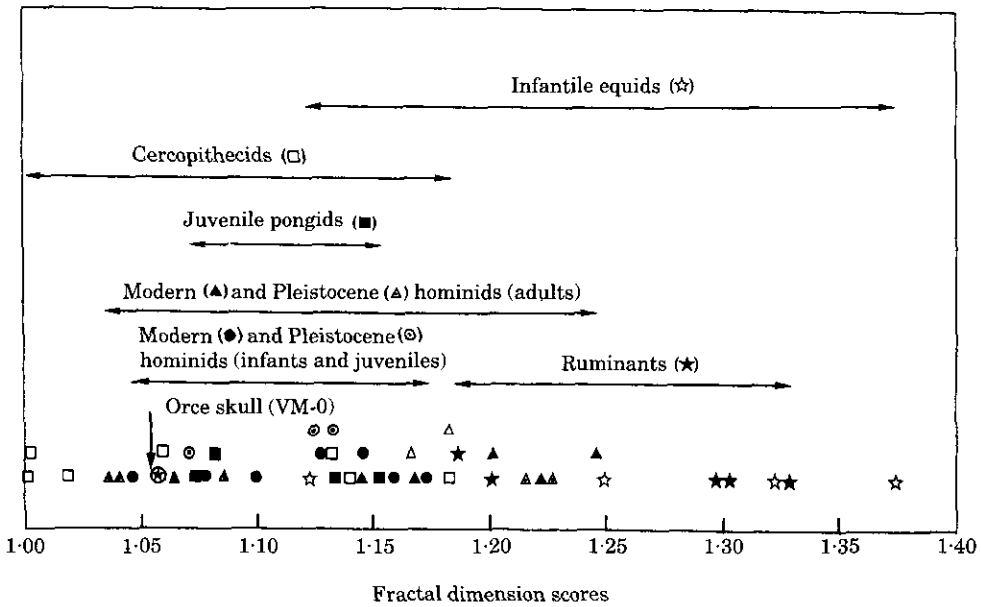
Figure 7. Plot of values and ranges of variation in fractal dimension (*D*) scores obtained in the analysed specimens and groups (data from Table 1).

It must be borne in mind that similarity of fractal dimension values associated with two particular skull sutures need not imply close taxonomical affinity; all that may be inferred is that both sutures share a similar degree of design complexity. Because similar fractal dimensions only imply similarity in design complexity, this morphometrical approach should perhaps be reserved for highlighting differences between specimens.

Results and discussion

Table 1 and Figure 7 present the values of the fractal dimension estimated from the sutures analysed for each specimen. It is noteworthy that the sagittal and right lambdoid sutures of the Venta Micena cranial fossil gave a fractal dimension (*D*=1·058) similar to those of equivalent sutures obtained from specimens belonging to modern and Plio-Pleistocene infant or adolescent hominids (*D*=1·047–1·173). Adult hominids have on average more complex sutures than infantiles and juveniles, which is reflected in their higher values of fractal dimension (*D*=1·037–1·246): it is interesting to note that adult lower Pleistocene members of the genus *Homo* fall either below or into the infant range of variation for modern humans. The fractal dimension associated with cercopithecids varied from 1·002–1·183. The pongids analysed, all of them juveniles, have values of fractal dimension (*D*=1·074–1·153) which are similar to those of infant hominids; adult pongid skulls have occipital and sagittal ridges which impede comparability with the Venta Micena cranial fragment, which lacks them (Gibert *et al.*, 1989*d*). Because Hartwig (1991) found there to be no correlation between bregma-lambda chord length and the degree of complexity of human sagittal sutures as reflected in their fractal dimension, it is reasonable to infer that the value of the fractal dimension (*D*=1·058) for the sutural regions preserved in the Venta Micena fossil lies

quite close to the value of the fractal dimension that the missing parts of the sutures would have afforded.

Both of the non-primate mammalian groups analysed gave noticeably higher values for the fractal dimension than those of infant hominids, young pongids or cercopithecids. In equids, relative complexity of the sagittal and right lambdoid sutures increases with ontogenetical development: values for the fractal dimension increase with biological age and the only equid value in the infant hominid range comes from an equid less than 1 month old (specimen 6933, $D=1\cdot123$). Not only was its sagittal suture almost linear, but also other important morphological differences between this specimen and both the Venta Micena skull fragment and modern and fossil infant hominids involve parietal bone thickness, transverse curvature measured from the obelion, longitudinal curvature over the length of the sagittal suture, and its lambdoid angle (Gibert *et al.*, 1989*a,c,d*). It is very important to realize that if newborn equids, such as specimen 6933, exhibit a fractal dimension that is equal to, or higher than those of infant hominids, such as the Venta Micena skull, then with advancing biological age substantial differences will increasingly separate the corresponding cranial sutures of *Equus* from those of *Homo*. It is surely significant that analysis of the other equids—all herbivores, of course—gave considerably higher values for the fractal dimension ($D=1\cdot249-1\cdot374$) than did the primates. The average value of the fractal dimension of infant and adolescent hominid sutures ($D=1\cdot117$, S.D.$=0\cdot041$, $n=10$) is significantly lower than the equivalent average for young equids ($D=1\cdot267$, S.D.$=0\cdot109$, $n=4$) when Student's t-test is applied ($t=2\cdot68$, df$=12$, $P<0\cdot05$; one-tail test). Because the data depart from a statistically normal distribution, as may be appreciated from Table 1, the non-parametric Mann-Whitney U test (Sprent, 1989) was also applied and provided a statistically significant result ($U=7$, $P<0\cdot05$). The various ruminants studied gave fractal dimensions for their skull sutures ($D=1\cdot186-1\cdot329$) which, although not exactly comparable, were higher than those obtained in primates.

To judge from the results, the fractal dimension of the skull sutures that are preserved in the fragment of occipital bone found at the Venta Micena site, separates it from equid crania. Nevertheless, using this criterion alone the possibility cannot be ruled out that it might have formed part of the cranial vault of some other primate. The complexity of sutures seen in infant hominids is not very different from that seen in young pongids and cercopithecids. However, there are other distinctive morphological differences between cercopithecid crania and the Venta Micena skull (Gibert *et al.*, 1989*d*). These differences include: (a) presence in adult cercopithecids of high sagittal ridges in the nape; (b) lower cercopithecid cranial capacity; (c) very low transverse and longitudinal vault curvatures in cercopithecids; and (d) very wide angle at the lambdoid suture. As for pongids, they have left no fossil traces in the European Plio-Pleistocene; they became extinct in Europe during the Upper Miocene and were relegated to Africa and Asia.

Conclusions

The value of the fractal dimension (D) obtained from the cranial sutures preserved in the fragment of occipital bone found at the Venta Micena site lies within the range of values that were obtained from specimens belonging to infants of modern and Plio-Pleistocene hominids. They, in turn, display D values that are similar to D values obtained from the other primates considered in the study, namely, cercopithecids and young pongids.

The values of D estimated from the specimens of *Equus* included in the study are higher than the equivalent values for primates. Therefore, it is possible to state that, as regards the relative

complexity of its sutures, the skull fragment from Venta Micena could not have belonged to an equid (*pace* Agustí & Moyà-Solà, 1987).

In view not only of the presence of substantial anatomical differences between the Venta Micena skull and skulls of cercopithecids, but also of the absence of fossil pongids in the European Pliocene and Pleistocene, the value of D obtained from the sutures preserved in the Orce skull leads us to conclude that this fossil most probably belonged to an infant of *Homo* sp. This result is consistent with the suggestions of Gibert *et al.* (1989*a,c,d*), who attribute an age of between 5 and 6 years old to the individual. This estimate was based partly on the thickness of the bony vault and partly on the absence of any sign of sutural synostosis.

Acknowledgements

References

Agustí, J. & Moyà-Solà, S. (1987). About identity of the cranial fragment of 'Venta Micena' site (Orce, Granada, Spain) attributed to '*Homo sapiens*'. *Estudios Geológicos* **43,** 538–543.

Anadón, P., Julià, R., De Deckker, P., Rosso, J. C. & Solulié-Marsche, I. (1987). Contribución a la paleolimnologia del Pleistoceno inferior de la cuenca de Baza (sector de Orce-Venta Micena). *Paleontologia i Evolució,* Mem. Esp. **1,** 35–72.

Arsuaga, J. L., Martínez I., Gracia A., Carretero J. M. & Carbonell, E. (1993). Three new human skulls from the Sima de los Huesos Middle Pleistocene site in Sierra de Atapuerca, Spain. *Nature* **362,** 534–537.

Avnir, D., Farín, D. & Pfeifer, P. (1984). Molecular fractal surfaces. *Nature* **308,** 261–263.

Baker, G. L. & Gollub, J. P. (1990). *Chaotic Dynamics, An Introduction.* Cambridge: Cambridge University Press, 182 pp.

Barnsley, M. (1988). *Fractals Everywhere.* Boston: Academic Press.

Bayer, U. (1985). Pattern recognition problems in geology and paleontology. *Lecture Notes in Earth Sciences 2.* London: Springer-Verlag.

Black, D. (1930). On an adolescent skull of *Sinanthropus pekinensis* in comparison with an adult skull of the same species and with other hominid skulls recent and fossils. Geological Survey of China, Series D. Vol. VII, fascicle II.

Borja, C., García-Pacheco, J. M., Ramírez-López, J. P. & García-Olivares, E. (1992). Cuantificación y caracterización de la albúmina fósil del cráneo de Orce. In (Ayuntamiento de Orce, Ed.) *Proyecto Orce-Gueva Victoria (1988–1992): Prescencia Humana en el Pleistoceno Inferior de Granada y Murcia,* pp. 415–424.

Boyajian, G. E. & Lutz, T. (1992). Evolution of biological complexity and its relation to taxonomic longevity in the Ammonoidea. *Geology* **20,** 983–986.

Bradbury, R. H., Reichelt, R. E. & Green, D. G. (1984). Fractals in ecology: methods and interpretation. *Marine Ecology* **14,** 295–296.

Braddy, R. M. & Ball, R. C. (1984). Fractal growth of copper electrodeposits. *Nature* **309,** 225–229.

Burlando, B. (1990). The fractal dimension of taxonomic systems. *J. Theoret. Biol.* **146,** 99–114.

Burrough, P. A. (1981). Fractal dimensions of landscapes and other environmental data. *Nature* **204,** 240–242.

Caddy, J. F. & Stamatopoulos, C. (1990). Mapping growth and mortality rates of crevice-dwelling organisms onto a perforated surface: the relevance of "cover" to the carring capacity of natural and artificial habitats. *Est. Coast Shelf Sci.* **31,** 87–106.

Caldwell, C. B., Stapleton, S. J., Holdsworth, D. W., Jong, R. A., Weiser, W. J., Cooke, G. & Yaffe, M. J. (1990). Characterization of mammographic parenchymal pattern by fractal dimension. *Phys. Med. Biol.* **35,** 235–247.

Campillo, D. 1989. Estudio del hombre de Orce. In (Gibert, J., Campillo, D. & García Olivares, Eds) *Los Restos Humanos de Orce y Cueva Victoria*, pp. 187–220. Sabadell: Institut Paleontològic Dr M. Crusafont, Diputació de Barcelona.

Cecca, F. (1992). Ammonite habitats in the Early Tithonian of Western Tethys. *Lethaia* **25**, 257–267.

Damiani, G. (1990). Computer simulation of some ammonoid suture lines. In (G. Pallini, F. Cecca, S. Cresta & M. Santantonio, Coords.) *Atti II Convengo Internationale: Fossili, Evoluzione, Ambiente*, pp. 221–228. Pergola.

Dicke, M. & Burrough, P. A. (1988). Using fractal dimensions for characterizing tortuosity of animal traits. *Physiolog. Entomol.* **13**, 393–398.

Feder, J. (1988). *Fractals*. New York: Plenum Press.

Fluegeman, R. H. & Scott-Snow, R. (1989). Fractal analysis of long-range paleoclimatic data: oxygen isotope record of Pacific core V28-239. *Pageoph.* **131**, 307–313.

Frontier, S. 1987. Applications of fractal theory in ecology. In (P. Legendre & L. Legendre, Eds) *Developments in Numerical Ecology*. Berlin: Springer-Verlag.

García-Ruíz, J. M., Checa, A. & Rivas, P. (1990). On the origin of ammonite sutures. *Paleobiol.* **16**, 349–354.

Gibert, J. 1986. El yacimiento de Venta Micena (Orce, Granada): su importancia, acción antropológica y caracteristicas paleoantropológicas del fragmento de cráneo de *Homo* sp. In (O. Arteaga, Ed.) *Homenaje a Luis Siret (1934 a 1984). Actas del congreso "Homenaje a Luis Siret, Cuevas de Almanzora, Junio 1984*, pp. 37–49. Madrid: Dirección General de Bellas Artes de la Consejería de Cultura de la Junta de Andalucía.

Gibert, J. & Palmqvist, P. (1992). Dimensión fractal de las suturas del cráneo de Orce. *Rev. Esp. Paleontol.* **7**, 154–160.

Gibert, J., Ruz, C. & Ribot, F. (1986). Human origin of the cranial fragment of 'Orce'. *Comunicacions II Jornades de Paleontologia i Evolució*, Sabadell **20**, 169–178.

Gibert, J., Campillo, D., Caporicci, R., Ribot, F., Ferrández, C. & Martínez, B. (1989a). Anatomical study: comparison of the hominid cranial fragment from Venta Micena (Orce, Spain) with fossil and extant mammals. *Hum. Evol.* **4**, 283–305.

Gibert, J., Martínez, B., Caporicci, R., Jiménez, C., Ferrández, C., Ribot, F., Soria, F. J., Pérez-Cuadrado, J. L., Arribas, A., Canals, J., Garcia-Targa, J. M., Iglesias, A. & Romero, R. (1989b). *Resumen de la investigaciones paleoantropológicas y arqueológicas de Orce (Granada) y Cueva Victoria (Cartagena) COL-PA* **42**, 11–60.

Gibert, J., Ribot, F., Ferrández, C., Martínez, B. & Caporicci, R. (1989c). Características diferenciales entre le fragmento de cráneo de Homo sp. de Venta Micena (Orce, Granada) y los équidos. *Estud. Geológ.* **45**, 121–138.

Gibert, J., Ribot, F., Ferrández, C., Martínez, B. & Ruz, C. (1989d). Diagnosis diferencial del fragmento del cráneo de *Homo* sp. del yacimiento de Venta Micena (Orce, Granada). In (J. Gibert, D. Campillo & E. García Olivares, Eds) *Los Restos Humanos de Orce y Cueva Victoria*, pp. 31–108. Sabadell: Institut Paleontòlogic Dr M. Crusafont, Diputació de Barcelona.

Gibert, J., Arribas, A., Martínez, B., Albadalejo, S., Gaete, R., Gibert, L., Peñas, C. & Torrico, R. (1992). Sintesis cronoestratigráfica del Pleistoceno inferior de la región de Orce. In (J. Gibert, Coord.) *Proyecto Orce-Cueva Victoria (1988–1992): Presencia humana en el Pleistoceno inferior de Granada y Murcia*, pp. 107–114. Granada: Ayuntamiento de Orce.

Gibert, J., Arribas, A., Martínez, B., Albadalejo, S., Gaete, R., Gibert, L., Oms, O., Peñas, C. & Torrico, R. (1994). Biostratigraphie et Magnetostratigraphie des gisements a presence humaine et action anthropique du Pleistocene inferieur de la region d'Orce (Granada, Espagne). *Comptes Rendus* **318**, 1277–1282.

Glenny, R. W., Robertson, H. T., Yamashiro, S. & Bassingthwaighte, J. B. (1991). Applications of fractal analysis to physiology. *J. Appl. Physiol.* **70**, 2351–2367.

Hartwig, W. C. (1991). Fractal analysis of sagittal suture morphology. *J. Morphol.* **210**, 289–298.

Horsfield, K. (1990). Diameters, generations, and orders of branches in the bronchial tree. *J. Appl. Physiol.* **68**, 457–461.

Howell, C. & Coppens, Y. (1976). An overview of hominidae from the Omo succession, Ethiopia. In (E. Coppens, F. C. Howell, G. Isaac & R. Leakey, Eds) *Earliest Man and Environments in the Lake Rudolf Basin. Prehistoric Archaeology and Ecology Series*. University Chicago: Chicago Press.

Hoyez, B. (1992). Analyse fractale de la forme des grains de sable. *Comptes Rendus Acad. Sci. Paris* **314**, 945–951.

Jacob, T. (1967). Recent Pithecanthropus finds in Indonesia. *Curr. Anthrop.* **8**, 501–504.

Jakeman, E. (1984). Scattering by fractal objects. *Nature* **307**, 110–111.

Kent, C. & Wong, J. (1982). An index of littoral zone complexity and its measurement. *Can. J. Fish. Aquat. Sci.* **39**, 847–853.

Leakey, R. E. F., Butzer, K. W. & Day, M. H. (1969). Early *Homo sapiens*. Remains from the Omo River Region of South-West Ethiopia. *Nature* **222**, 1132–1138.

Lochle, C. (1983). The fractal dimension in ecology. *Spec. Sci. Tech.* **6**, 131–142.

Long, C. A. (1985). Intricate sutures as fractal curves. *J. Morphol.* **185**, 285–295.

Lovejoy, S. (1982). Area–perimeter relation for rain and cloud areas. *Science* **216**, 185–187.

Lynch, J. A., Hawkes, D. J. & Buckland-Wright, J. C. (1991). Analysis of texture in microradiographs of osteoarthritic knees using fractal signatures. *Phys. Med. Biol.* **36**, 709–722.

Mandelbrot, B. B. (1967). How long is the coast of Britain? Statistical self-similarity and fractional dimensions. *Science* **156,** 636–638.

Mandelbrot, B. B. (1983). *The Fractal Geometry of Nature.* New York & San Francisco: W. H. Freeman.

Martínez, B. (1991). Revisión sistemática y estudio cuantitativo de la fauna de macromamíferos del yacimiento de Venta Micena. Ph.D. Thesis, University of Barcelona.

Matsuyama, T., Sogawa, M. & Nakagawa, Y. (1989). Fractal spreading growth of *Serratia marcescens* which produces surface active exolipids. *FEMS Microbiol. Lett.* **61,** 243–246.

McKinney, M. L. & Frederik, D. (1992). Extinction and population dynamics: new methods and evidence from Paleogene foraminifera. *Geology* **20,** 343–346.

Mendoza, M., Palmqvist, P., Guerrero, S., Martínez, B., Pérez Claros, J. A., Gibert, J. & Eisenmann, V. (1993). Consideraciones tafonómicas, paleoecológicas y paleoetológicas sobre la comunidad de macromamíferos de Venta Micena (Orce, Granada). In (J. M. González Donoso, Ed.) *Comunicaciones IX Jornadas de Paleontología*, pp. 73–78. Málaga.

Moore, R. C. (Ed.) (1975). *Treatise on Invertebrate Paleontology. Part L. Mollusca 4 (Ammonoidea).* Boulder, Colorado: University of Kansas Press & The Geological Society of America.

Morse, D. R., Lawton, J. M., Dodson, M. M. & Williamson, M. H. (1985). Fractal dimension of vegetation and the distribution of arthropod body lengths. *Nature* **314,** 731–733.

Nittman, J., Daccord, G. & Stanley, H. E. (1985). Fractal growth of viscous fingers: quantitative characterization of a fluid instability phenomenon. *Nature* **314,** 141–144.

Obert, M., Pfeifer, P. & Sernetz, M. (1990). Microbial growth patterns described by fractal geometry. *J. Bacteriol.* **172,** 1180–1185.

Olóriz, F. & Palmqvist, P. (1995). Sutural complexity and bathymetry in ammonites: fact or artifact? *Lethaia* **28** (in press).

Palmer, M. W. (1988). Fractal geometry: a tool for describing spatial patterns of plant communities. *Vegetatio*, **75,** 91–102.

Palmqvist, P., Gibert, J. & Martínez, B. (1992). Sobre la relación tamaño/abundancia en los macromamíferos de Venta Micena y sus implicaciones tafonómicas. *Rev. Españ. Paleontol.* **7,** 174–180.

Peitgen, H. & Saupe, D. (1988). *The Science of Fractal Images.* New York: Springer-Verlag.

Pennycuick, C. J. & Klein, N. C. (1986). Units of measurement for fractal extent, applied to the coastal distribution of bald eagle nests in the Aleutian Islands, Alaska, *Oecologia* **68,** 254–258.

Phillips, J. D. (1985). Measuring complexity of environmental gradients. *Vegetatio* **64,** 95–102.

Plotnik, R. (1986). A fractal model for the distribution of stratigraphical hiatuses. *J. Geol.* **94,** 885–890.

Plotnik, R. (1988). A fractal model for the distribution of stratigraphical hiatuses; a reply. *J. Geol.* **96,** 102–103.

Reyment, R. A. (1991). *Multidimensional Palaeobiology.* Oxford: Pergamon Press.

Ritz, K. & Crawford, J. (1990). Quantification of the fractal nature of colonies of *Trichoderma viride. Mycolog. Res.* **94,** 1138–1152.

Sernetz, M., Gelléri, B. & Hofmann, J. (1985). The organism as a bioreactor. Interpretation of the reduction law of metabolism in terms of heterogeneous catalysis and fractal structure. *J. Theoret. Biol.* **117,** 209–230.

Sander, L. M. (1986). Fractal growth processes. *Nature* **322,** 789–793.

Slice, D. E. (1989). *Fractal-D.* New York: Exeter Publishing Co.

Slice, D. E. (1993). The fractal analysis of shape. In (L. F. Marcus, E. Bello & A. García-Valdecasas, Eds) *Contributions to Morphometrics*, Vol. 8. pp. 161–190. Madrid: monografías del Museo Nacional de Ciencias Naturales.

Sprent, P. (1989). *Applied Nonparametric Statistical Methods.* London: Chapman & Hall.

Stringer, C. B. (1974). A multivariate study of the Petralona Skull. *J. hum. Evol.*

Sugihara, G. & May, R. (1990). Applications of fractal in ecology. *Trends Ecol. Evol.* **5,** 79–86.

Tatsumi, J., Yamanchi, A. & Kono, Y. (1989). Fractal analysis of plant root systems. *Ann. Bot.* **64,** 499–503.

Tobias, P. V. (1991). *Olduvai Gorge. The Skulls Endocasts and Teeth of* Homo habilis, Vol. 4. Cambridge: Cambridge University Press.

Vera, J. A., Fernández, J., López Garrido, A. C. & Rodríguez Fernández, J. (1985). Geología y estratigrafía de los materiales pliocenos-pleistocenos del sector de Orce-Venta Micena (Prov. Granada). *Paleontol. Evol.* **18,** 3–11.

Vlecek, J. & Cheung, E. (1986). Fractal analysis of leaf shapes. *Can. J. Forest Res.* **16,** 124–127.

West, B. J. & Goldberger, A. L. (1987). Physiology in fractal dimensions. *Am. Sci.* **75,** 354–365.

Wood, B. (1991). *Koobi Fora Research Project*, Vol. 4. Oxford: Clarendon Press.